

Piotr Więcek,  
\*Miroslaw Polipowski,  
Boguslaw Więcek

Faculty of Electrical, Electronic, Computer and  
Control Engineering  
Lodz University of Technology,  
ul. B. Stefanowskiego 18/22, 90-924 Łódź, Poland

\*Textile Research Institute,  
ul. Brzezińska 5/15, 92-103 Łódź, Poland

# Stereovision System for 3D Analysis of the Geometrical Properties of Fabrics

## Abstract

In this paper, a stereovision system for measuring the geometrical properties of fabrics is presented. Measurement of the parameter of spacings between the yarns is the main application of the system proposed. The algorithms implemented are described in detail which explain how one can measure the area of the front of the spacing as well as its orientation in a 3D space. The calibration procedure, using a specially prepared calibrator, is outlined. An accuracy analysis is presented both for the area and angle measurements. Exemplary results of measuring the areas and angles for 100 spacings between the yarns are presented in the form of histograms and tables.

**Key words:** stereovision, direct linear transformation (DLT), 3D analysis, geometrical properties, non-destructive testing.

## Introduction

Nowadays progress in information technology allows to implement novel techniques either in research or in many practical and industrial applications, one of example of which is the 3D stereovision imaging of different objects. In textile technology digital imaging, including stereovision, is now being used mainly

for textile material characterisation [3, 6, 8, 13]. Most involve 2D imaging using a single camera [4], but more and more 3D imaging is applied [3, 6, 8, 13]. A typical application of 3D imaging is full body scanning for cloth designing [8, 13]. These applications are rather suited to the macro scale, are fast, in real-time and already commercially used [12]. For the micro scale there are fewer systems available due to the complex setup of the apparatus that includes stereo microscopes as well as dedicated and calibrated optical components. In this domain, photogrammetric methods are used for 3D object reconstruction [1, 2, 10, 11], many of which are based on the well-known *Direct Linear Transformation (DLT)*, widely used in photogrammetry, geodesy and remote sensing [2, 11].

In this paper we present a 3D stereovision system made for investigation of the geometric properties of fabrics on a micro scale using a 2-camera imaging system equipped with a zoom lens and ring extender for appropriate magnification of the images. The *DLT* was implemented for spatial reconstruction of the fabric structure and measuring the dimensions, area and orientation of the spacings between the yarns. The final aim of the research is a new method of evaluation of the area of the spacings, the moisture, vapour, air and partially radiation transfer through the fabric using the geometric properties of the channels, spacings and yarns measured using the stereovision system. Such measurements can be implemented in the form of an expert system, e.g. an artificial neural network can be used to approximate the relationship between the fabric's properties and its technological and 3D structural parameters. The aim of this research was to elaborate a new

non-destructive method for estimation of the structure and physical parameters of textile. Measurement of the area and orientation of the front input of the spacing in a 3D space was one of the main aims of this research.

## Stereovision system for 3D reconstruction

The stereovision system dedicated for fabric measurements consists of 2 standard CCD cameras located on a tripod (*Figure 1*). The cameras are fixed mechanically. In this research program methods and software for 3D reconstruction were elaborated. The hardware of the system was made during the previous investigation, which was mainly dedicated for 2D textile characterisation [4]. It determines the distance  $d$  (the so-called *base*) between them as well as the given orientation in a 3D space (localisation of cameras' optical axis). The cameras have the possibility of movement in the  $z$  (vertical) direction. The object is placed below the cameras on a table, which can move in the  $x$  and  $y$  directions with a micrometer resolution. There is back and

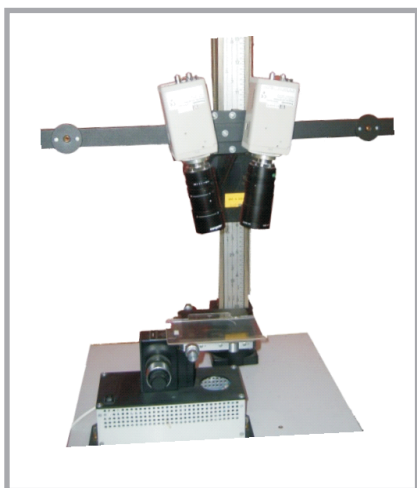


Figure 1. Stereovision 3D reconstruction.

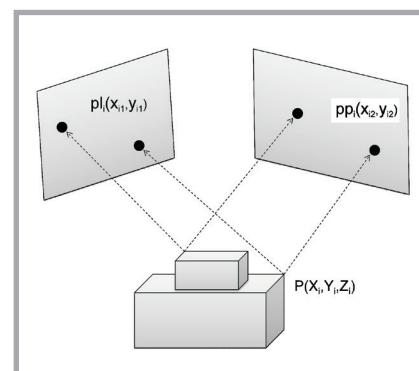


Figure 2. Principle of 3D coordinate measurement.

side illumination of the object located on the table, as shown in **Figure 1**.

The system is typically used for 3D coordinate measurement of selected points on a fabric. In order to calculate these coordinates, the operator needs to recognise and locate the same points in both the left and right images – **Figure 2**. At this stage of the research, the measuring points are defined manually. The operator uses a pointer on the screen to define the same points in both images. In the system presented, the coordinates of yarns and spacings can be defined with a subpixel resolution up to 1/16 of the pixel size. Here it must be emphasised that 3D reconstruc-

tion of the object investigated strongly depends on the accuracy of determining the same points in both images. In addition, the cameras are equipped with a macro zoom varying the focal length of the lens, allowing to magnify the image to be large enough to identify the same points correctly in the images generated by both cameras.

A *Direct Linear Transformation* algorithm is implemented in the system presented. According to 3D reconstruction theory [2, 11], the  $i$ -th point coordinates of the left  $(x_{i1}, y_{i1})$  and right  $(x_{i2}, y_{i2})$  im-

ages are the functions of 3D space coordinates  $(X_i, Y_i, Z_i)$  – **Equations 1 and 2**.

$$\begin{aligned} x_{i1} &= \frac{A_1 X_i + B_1 Y_i + C_1 Z_i + D_1}{E_1 X_i + F_1 Y_i + G_1 Z_i + 1} \\ y_{i1} &= \frac{H_1 X_i + I_1 Y_i + J_1 Z_i + K_1}{E_1 X_i + F_1 Y_i + G_1 Z_i + 1} \end{aligned} \quad (1)$$

$$\begin{aligned} x_{i2} &= \frac{A_2 X_i + B_2 Y_i + C_2 Z_i + D_2}{E_2 X_i + F_2 Y_i + G_2 Z_i + 1} \\ y_{i2} &= \frac{H_2 X_i + I_2 Y_i + J_2 Z_i + K_2}{E_2 X_i + F_2 Y_i + G_2 Z_i + 1} \end{aligned} \quad (2)$$

Both **Equations 1 and 2** contain 11 unknown coefficients. Coefficients  $A_1, B_1, C_1, D_1, E_1, F_1, G_1, H_1, I_1, J_1$  &  $K_1$  correspond to the left and  $A_2, B_2, C_2, D_2, E_2, F_2, G_2, H_2, I_2, J_2$  &  $K_2$  to the right image. The values of these coefficients are determined in the calibration procedure presented below [2, 11].

### Calibration

In order to calculate the values of 11 unknown parameters of *DLT* for each of the 2 cameras ( $A_1, B_1, C_1, D_1, E_1, F_1, G_1, H_1, I_1, J_1$  &  $K_1$  and  $A_2, B_2, C_2, D_2, E_2, F_2, G_2, H_2, I_2, J_2$  &  $K_2$ ), the set of linear **Equations 3 and 4** has to be solved, defined for at least 6 reference points, for which one needs to know the coordinates in the 3D space  $(X_i, Y_i, Z_i)$  for  $i = 1, 2, \dots, 6$ .

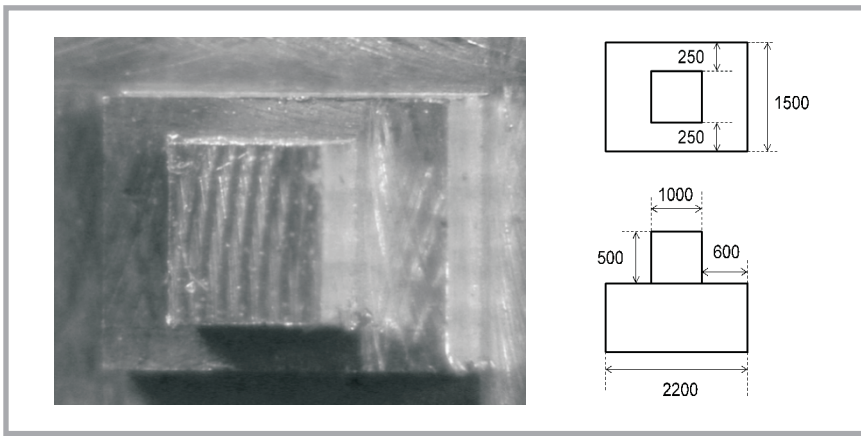


**Figure 3.** 3D stereovision calibrator (dimensions in  $\mu\text{m}$ ).

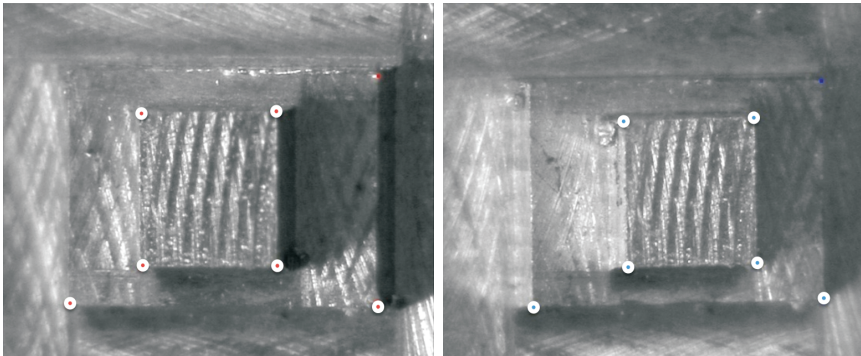


**Figure 4.** Left and right image of the calibrator with the reference points.

$$\begin{aligned} A_1 X_i + B_1 Y_i + C_1 Z_i + D_1 - E_1 x_{i1} X_i - F_1 x_{i1} Y_i - G_1 x_{i1} Z_i &= -x_{i1} \\ H_1 X_i + I_1 Y_i + J_1 Z_i + K_1 - E_1 y_{i1} X_i + F_1 y_{i1} Y_i + G_1 y_{i1} Z_i &= -y_{i1} \end{aligned} \quad (3)$$

$$\begin{aligned} A_2 X_i + B_2 Y_i + C_2 Z_i + D_2 - E_2 x_{i2} X_i - F_2 x_{i2} Y_i - G_2 x_{i2} Z_i &= -x_{i2} \\ H_2 X_i + I_2 Y_i + J_2 Z_i + K_2 - E_2 y_{i2} X_i + F_2 y_{i2} Y_i + G_2 y_{i2} Z_i &= -y_{i2} \end{aligned} \quad (4)$$

$$\begin{aligned} (A_1 - E_1 x_{i1}) X_i + (B_1 - F_1 x_{i1}) Y_i + (C_1 - G_1 x_{i1}) Z_i &= -(D_1 - x_{i1}) \\ (H_1 - E_1 y_{i1}) X_i + (I_1 - F_1 y_{i1}) Y_i + (J_1 - G_1 y_{i1}) Z_i &= -(K_1 - y_{i1}) \\ (A_2 - E_2 x_{i2}) X_i + (B_2 - F_2 x_{i2}) Y_i + (C_2 - G_2 x_{i2}) Z_i &= -(D_2 - x_{i2}) \\ (H_2 - E_2 y_{i2}) X_i + (I_2 - F_2 y_{i2}) Y_i + (J_2 - G_2 y_{i2}) Z_i &= -(K_2 - y_{i2}) \end{aligned} \quad (5)$$

**Equations 3, 4 and 5.**

In order to calibrate the system, a 3D solid (calibrator) was made – **Figure 3**, whose size was chosen according to the field of view of the cameras and size of spacings and yarns of the fabric used in the research. The accuracy of the calibrator's dimensions was achieved at the level  $\pm 20 \mu\text{m}$ .

The calibration procedure is rather straightforward. The operator indicates a minimum of 6 reference points in the left and right images. For more than 6 reference points, the least square method is used for solving (3) and (4). Two methods of calibration were used in the software – the standard *DLT* and so called *MDLT* (*Modified Direct Linear Transformation*) algorithms. Originally the *DLT* contained 10 independent parameters, not 11, as shown in **Equations 1 and 2**, which means that one can solve the sets of linear **Equations 3 and 4** with 10 parameters only, by eliminating one. Using *MDLT*, the 11<sup>th</sup> parameter is calculated iteratively using the non-linear relation in between them [11]. In this research we used the classical *DLT* approach. In order to determine constants  $A_1 - K_1$  and

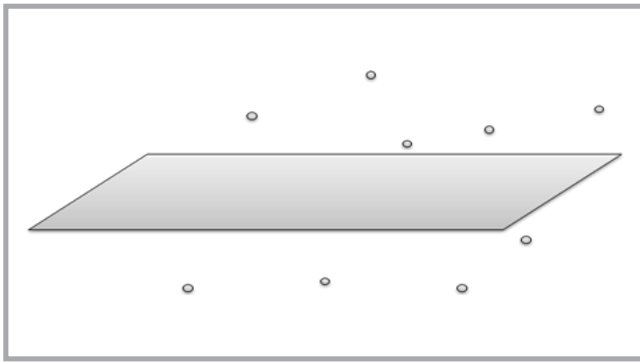


**Figure 5.** Measuring points and plane surface used for estimation of the area and orientation of the front of the spacing.

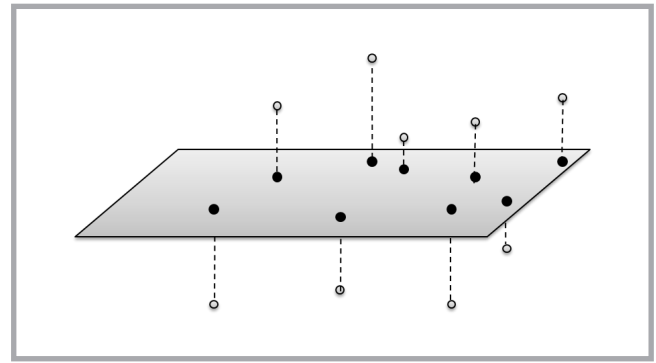


**Figure 7.** Projections of measuring points on the surface of the front of the spacing.

$A_2 - K_2$  we implemented the Gauss elimination for solving the linear set of **Equations 3 and 4**.

After getting values  $A_1 - K_1$  and  $A_2 - K_2$ , it is recommended to verify the correctness of the calibration by measuring one or more other reference points, e.g. other vertexes of the calibrator, with known values of 3D coordinates (**Figure 4**).

### 3D reconstruction

3D reconstruction entails the calculation of 3D space coordinates ( $X_i, Y_i, Z_i$ ) using 2D coordinates of the points from the left and right images. It can be performed using the set of 4 linear **Equations 5**.

In our case the operator recognises the same points in both images, and then the system calculates 3D coordinates ( $X_i, Y_i, Z_i$ ).

### Algorithms implemented for fabric characterisation

The different constructions of fabric determine the different spacings between yarns. The operator working with the system starts by selecting measuring

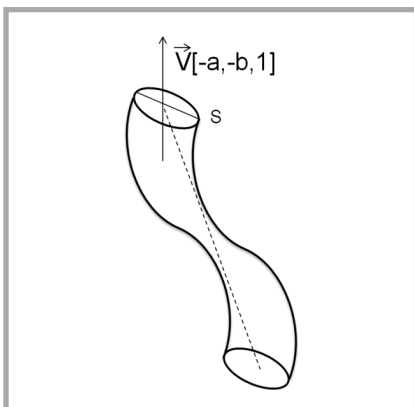


**Figure 6.** Vector perpendicular to the surface of the spacing.

points on the edge of the spacing manually. These points have to be chosen very carefully in both the left and right images. The accuracy of selecting the same points in both images determines the accuracy of the overall procedure of measuring the spacings' parameter, such as the area and orientation in a 3D space. In the next step of the research we plan to select the measuring point automatically using the matching procedures [2, 10].

### Plane surface of the front of the spacing

The plane surface of the front of the spacing is defined as a surface which divides the measuring points into 2 groups lying on both sides of the surface at the closest distance with respect to the minimum mean square error – **Figure 5**. According to analytical geometry, the equation of the plane surface can be presented in the general or directional forms as in **Equation 6**.

$$Ax + By + Cz + D = 0 \quad (6)$$

$$z = ax + by + c$$

The values of coefficients  $a, b, c$  of the plane surface of the front of the spacing are determined using linear regression (7).

$$\sum_{k=1}^N (z_i - ax_i + by_i + c)^2 = \min \quad (7)$$

where  $N$  in the number of measuring points.

The set of linear equations used for calculating values  $a, b$  &  $c$  takes the form (8). Coefficients of the plane surface defined in the general form are  $A = a, B = b, C = -1$  and  $D = c$ .

$$\begin{aligned} a \sum_{i=0}^{N-1} x_i^2 + b \sum_{i=0}^{N-1} x_i y_i + c \sum_{i=0}^{N-1} x_i &= - \sum_{i=0}^{N-1} x_i z_i \\ a \sum_{i=0}^{N-1} x_i y_i + b \sum_{i=0}^{N-1} y_i^2 + c \sum_{i=0}^{N-1} y_i &= - \sum_{i=0}^{N-1} y_i z_i \\ a \sum_{i=0}^{N-1} x_i + b \sum_{i=0}^{N-1} y_i + cN &= - \sum_{i=0}^{N-1} z_i \end{aligned} \quad (8)$$

### Vector perpendicular to the surface of the spacing

The vector perpendicular to the surface of the spacing is defined directly from the equation of the surface and can be presented as  $V = [-a, -b, 1]$ , **Figure 6**.

### Area of the front of the spacing

The area of front of the spacing can be determined after projections of all measuring points on the plane's surface calculated according to the procedure presented above (**Figure 7**).

One can calculate the coordinates of the projected points using the lines perpendicular to the surface and crossing the given measuring points ( $X_i, Y_i, Z_i$ ). These

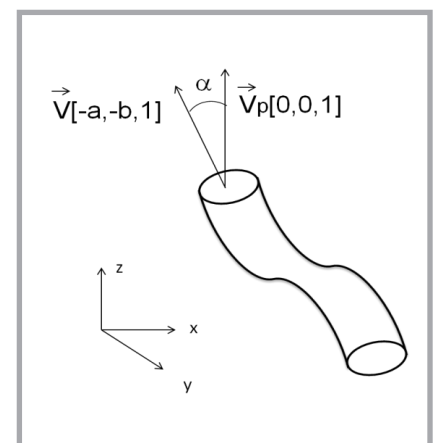


**Figure 8.** Angle between the normal to the surface and the vertical vector.

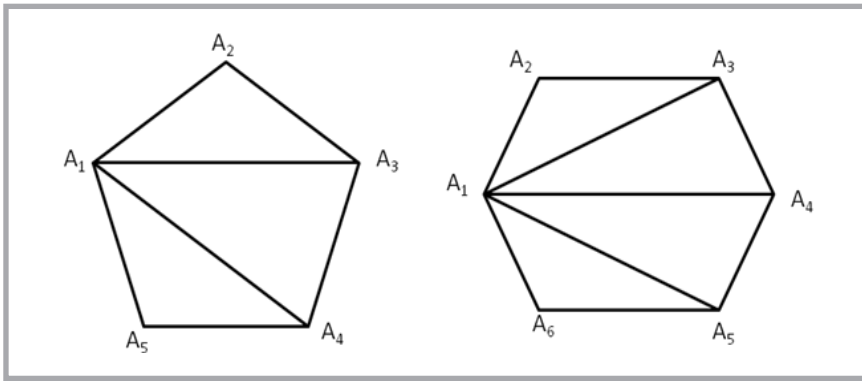


Figure 9. Polygonal front of the spacing between yarns divided into triangles.

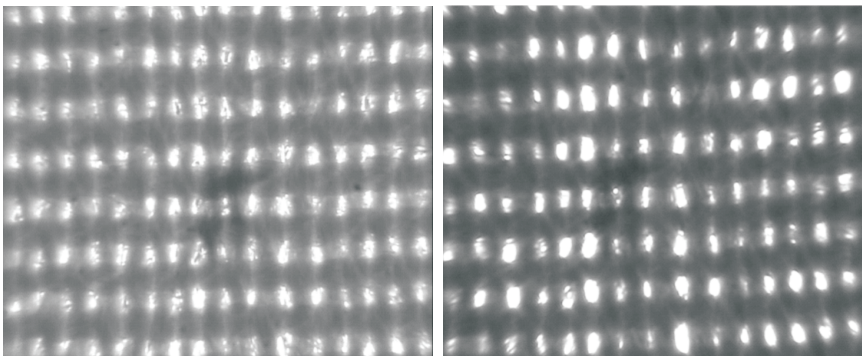


Figure 10. Fabric's images captured for 2D analysis.

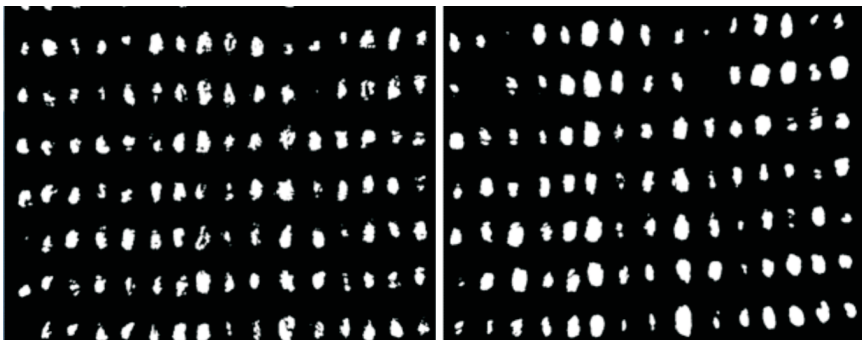


Figure 11. Binary images of the fabric.



Figure 12. Binary images after closing.

lines are easily presented using the parametric form.

$$\begin{aligned} x(t) &= X_i - at \\ y(t) &= Y_i - bt \\ z(t) &= Z_i - t \end{aligned} \quad (9)$$

The projection is calculated as the crossing point of the line with the surface. The value of parameter  $t$  defines this crossing point and is calculated as in (10).

$$\begin{aligned} Z_i + t &= a(X_i - at) + b(Y_i - bt) + c \\ t &= \frac{aX_i + bY_i - Z_i + c}{1 + a^2 + b^2} \end{aligned} \quad (10)$$

Finally the coordinates of the projected points  $(X_{pi}, Y_{pi}, Z_{pi})$  can be calculated using (11).

$$\begin{aligned} X_{pi} &= X_i - a \frac{aX_i + bY_i - Z_i + c}{1 + a^2 + b^2} \\ Y_{pi} &= Y_i - b \frac{aX_i + bY_i - Z_i + c}{1 + a^2 + b^2} \\ Z_{pi} &= Z_i + \frac{aX_i + bY_i - Z_i + c}{1 + a^2 + b^2} \end{aligned} \quad (11)$$

The projected points define a polygon. Measuring the area of the polygon is one of the main functions in the system. Each polygon describes the front side of the spacing in between the yarns. Firstly one divides the polygon into triangles. Then one measures the total area of the spacing as the sum of the areas of the triangles. One can notice that the number of non-overlapped triangles with one common vertex of the polygon is  $n = N - 2$ , where  $N$  denotes the number of polygon vertices – **Figure 9**.

The area  $S$  of the triangle can be easily calculated using the lengths of its edges  $(d_a, d_b, d_c)$  – **Equations 12**.

$$\begin{aligned} S &= \sqrt{p(p-d_a)(p-d_b)(p-d_c)} \\ p &= \frac{d_a + d_b + d_c}{2} \end{aligned} \quad (12)$$

#### The angle between the normal to the surface and the vertical vector

One of the very important parameters of the spacing between the yarns of the fabric is the angle between the normal to the surface and the vertical vector – **Figure 8** (see page 63). The value of the angle between vectors  $u[u_x, u_y, u_z]$  &  $v[v_x, v_y, v_z]$ , can be determined using their scalar product – **Equation 13**.

$$u \cdot v = u_x v_x + u_y v_y + u_z v_z = |u||v| \cos(\alpha) \quad (13)$$

Taking into account that the vectors between which we determine the angle have coordinates  $V = [-a, -b, 1]$  and  $V_p = [0, 0, 1]$ , the angle can be found using **Equation 14**

$$\cos(\alpha) = \frac{1}{\sqrt{a^2 + b^2 + 1}} \quad (14)$$

#### 2D approach for estimation of the relative area of spacings

The system presented allows 2D analysis of both left and right images of fabric. The method is based on morphological operations, binarisation and image seg-

Calibration file										
A	B	C	D	E	F	G	H	I	J	
1	Calibration file	D:\Textile3D_work\kalibracja\kalibracja8.txt								
2	Filename :	ch1-8.11.2013-10.52.46.bmp								
3	Left image:	no. of channels	132	white pixel:	10,285	threshold	187			
4	Right image:	no. of channels	121	white pixel:	10,954	threshold	162			
5										
6	Channel 1									
7	x-left	y-left	x-right	y-right	X	Y	Z	area	angle	
8	410		336	333	324	1002,776	631,2307	-954,353	7666,265	32,296
9	426		335	345	323	1068,847	641,4048	-999,436		
10	426		310	347	297	1074,363	746,595	-974,353		
11	413		312	336	299	1017,255	734,5205	-950,953		
12										
13	Channel 2									
14	x-left	y-left	x-right	y-right	X	Y	Z	area	angle	
15	460		338	392	325	1267,727	623,5273	-875,675	13039,57	28,404
16	481		336	408	323	1353,404	639,8085	-934,439		
17	477		310	402	294	1329,09	751,6128	-947,738		
18	458		311	384	296	1241,44	743,5668	-931,604		
19										
20	Channel 3									
21	x-left	y-left	x-right	y-right	X	Y	Z	area	angle	
22	474		383	397	366	1307,923	441,7482	-983,767	6109,303	15,978
23	475		417	403	401	1326,388	292,0353	-940,576		
24	459		416	386	401	1247,676	294,076	-944,14		

Figure 13. Fragment of the report of the exemplary experimental session.

mentation. Image preprocessing methods were implemented, such as erosion, dilatation and closing [7, 9]. The segmentation can be carried out manually using user-defined thresholds or automatically using e.g. the well-known Otsu method. The original images before segmentation are presented in Figure 10, while binary images before and after the morphological closing operation are shown in Figures 11 and 12. The ratio of the area of the spacings and the total image area is the result of 2D analysis of both the left and right images [4].

### Reporting

In addition, the system allows flexible reporting of research results and to export data in MS-Excel® format for further use. The report contains calibration data and the results of 2D and 3D image processing – Figure 13. The system saves 2D coordinates of selected pixels, coordinates of 3D reconstructed points, values of areas and angles of selected spacings. The system presented consists of 2 standard CCD cameras equipped with a zoom lens, a computer of sufficient power and software elaborated in this research. After optical adjustment of the cameras, the operator takes 2 still images and saves them on the computer, and then they run the program for 3D object reconstruction. The program asks the operator to indicate on the screen the same points in the images captured from

both cameras. Finally the software calculates the areas and orientation angles of the spacings selected and generates the results and reports.

## Preliminary experimental results

### Uncertainty of the measurements

The system for 3D analysis of fabric geometry consisted of 2 standard CCD

cameras (Figure 1) with a 1/3" sensor of 768 (H) × 492 (V) pixels, and was equipped with a variable focal length, macro zoom lens (10X) and an extender which increased the image size 2 times. The scanning area of the object for the minimum distance between the object and the camera was about 2.5 × 2.1 mm<sup>2</sup>. The image from the detector was pre-processed in the camera before sending to the computer as an analog signal. In addition, digitalisation of the image, made

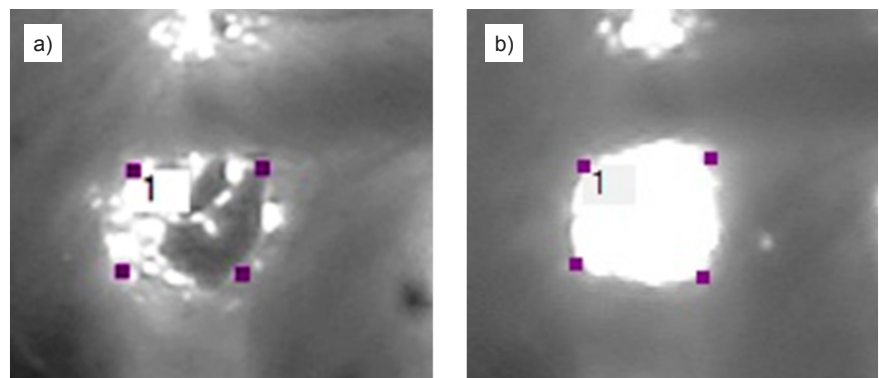


Figure 14. Exemplary spacing between yarns for fabric KM 1/150 selected for uncertainty estimation (a - left, b - right image).

Table 1. Results of 10 averaged measurements of the spacing presented in Figure 14.

	Area, μm <sup>2</sup>	Angle, °
Mean value	36137.1	11.6
Standard deviation	2651.4	3.6
Standard deviation for averaged 10 measurements	838.4	1.1

by the grabbers, gives a final resolution of the image of  $720 \times 576$ . Such a resolution determines the pixel area of the object. For the minimum distance between the camera and fabric, which is about 15 cm, the pixel area can be estimated as  $3.47 \times 3.65 \mu\text{m}^2$ . In practice, one never works at the minimum distance between the camera and the object.

Uncertainty analysis was applied to estimate the overall performance of the system. Extended standard uncertainty  $u$  consists of random (type A)  $u_A$  and systematic (type B)  $u_B$  uncertainty components – Equation 15.

$$u = k\sqrt{u_A^2 + u_B^2} \quad (15)$$

where  $k$  is the coverage factor dependent on the degree of freedom (the number of measurement results taken in the analysis minus 1) and the required level of confidence of the results obtained.

The standard uncertainty  $u_A$  of the system was evaluated by performing 10 measurements of a selected spacing – Figure 14. The results of measurement of both the area and angle of the spacing are presented in Table 1.

For the single measurement, the standard uncertainty was  $u_A = 2651.4 \mu\text{m}^2$ . If 10 measurement results were averaged, the uncertainty was scaled by factor  $1/N^{0.5}$ , which was  $u_A = 838.4 \mu\text{m}^2$ , where  $N$  was the number of measurement results taken for averaging.

The standard uncertainty  $u_B$  depends on the pixel size of the scanning area. During the measurements, the system was tuned to a pixel size of  $3.5 \times 3.7 \mu\text{m}^2$ . The average equipment-dependent uncertainty  $u_B$  for the distance measurement was estimated as [12]

$$u_B = \frac{3.6 \mu\text{m}}{\sqrt{3}} \approx 2.1 \mu\text{m} \quad (16)$$

For the area measurement, uncertainty  $u_B$  can be easily evaluated for different spacing shapes. The standard uncertainty  $u_B$  for a square spacing can be expressed as:

$$u_{B\text{square}} = 2au_B \approx 800 \mu\text{m}^2 \quad (17)$$

where  $a$  is the length of the square's side.

For the spacing in Figure 14, the side of the square approximated was estimated as  $a \approx 190 \mu\text{m}$ . According to Student's  $t$ -statistics, the coverage factor is typically selected from the range  $k \in (2, 3)$ . In the example presented above, we took  $N = 10$  measurement results for uncertainty analysis. It denotes that the coverage factor for confidence level  $p = 0.95$  is  $k = t_{9,0.95} = 2.3$ . Finally the extended standard uncertainty for area measurement of the spacing in Figure 14 for a single measurement took the value (18).

$$u = 2.3\sqrt{2651.4^2 + 800^2} = 6368 \mu\text{m}^2 \quad (18)$$

For 10 averaged results, the extended standard uncertainty decreased more than 2 times – Equation 19.

$$u = 2.3\sqrt{838.4^2 + 800^2} = 2371 \mu\text{m}^2 \quad (19)$$

From the uncertainty analysis presented here, one can conclude that the random uncertainty  $u_B$  has a major contribution. Standard uncertainties  $u_A$  and  $u_B$  became almost equal when we averaged 10 measurement results for each spacing. The highest relative value of the extended uncertainty for a single measurement was about 17.6% in the example presented, which is a quite satisfactory result if we take into account that the area measured was rather small in comparison to the entire area of the fabric visualised by the cameras.

Table 2. Statistical parameters of exemplary measurement of fabric 91/2009.

Parameter	Value
No. of channels	126
Mean area of the spacings	10,62 %
Left threshold	187
Right threshold	162
	<b>Area, <math>\mu\text{m}^2</math></b>
Min	2607
Max	19766
Mean	10510
Median	10770
Standard deviation	3457
	<b>Angle, <math>^\circ</math></b>
Min	1.69
Max	44.4
Mean	19.3
Median	19.3
Standard deviation	9.2

A similar analysis can be carried out for measurement of the angle. The standard uncertainty  $u_A$  can be evaluated using Equation 14, which is much easier to perform numerically. We assumed that for both the area and angle the extended standard uncertainty mainly depends on the random component  $u_B$ . With such an assumption, the extended standard uncertainty for the angle was estimated as  $u \approx u_B = 3.6^\circ$ . The relative uncertainty of the angle measurement was much worse in comparison to measurement of the area of the spacing. For the exemplary spacing presented in Figure 14, it varied from 21% up to 62%, meaning that if one requires better accuracy of measurement of the angle of the spacing, averaging is strongly recommended.

### Preliminary results

As an example of application of 3D stereovision system for characterisation of textiles, fabric 91/2009 was taken for measurements. In the field of view of the

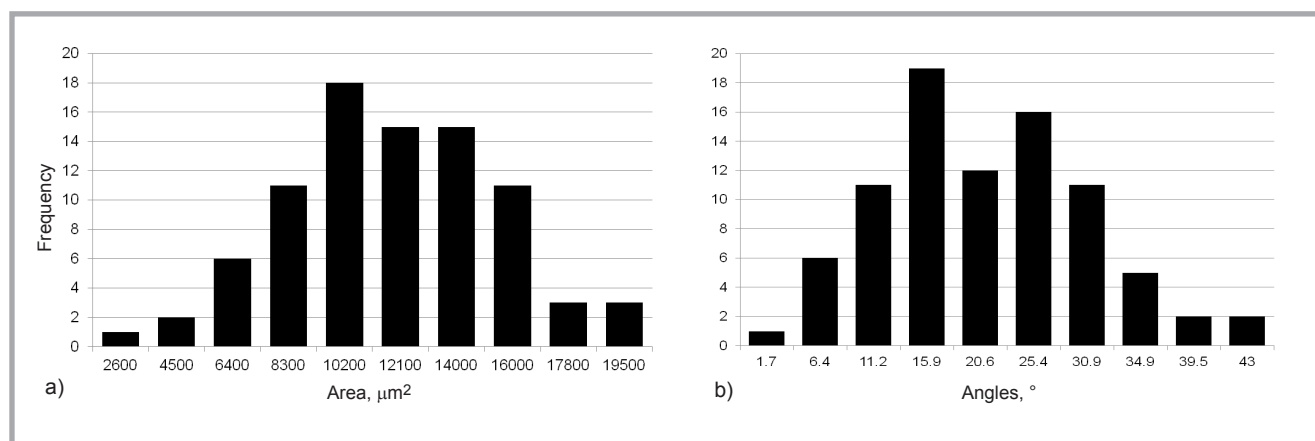


Figure 15. Histogram of: a) area and b) angles measurements for fabric no. 91/2009.

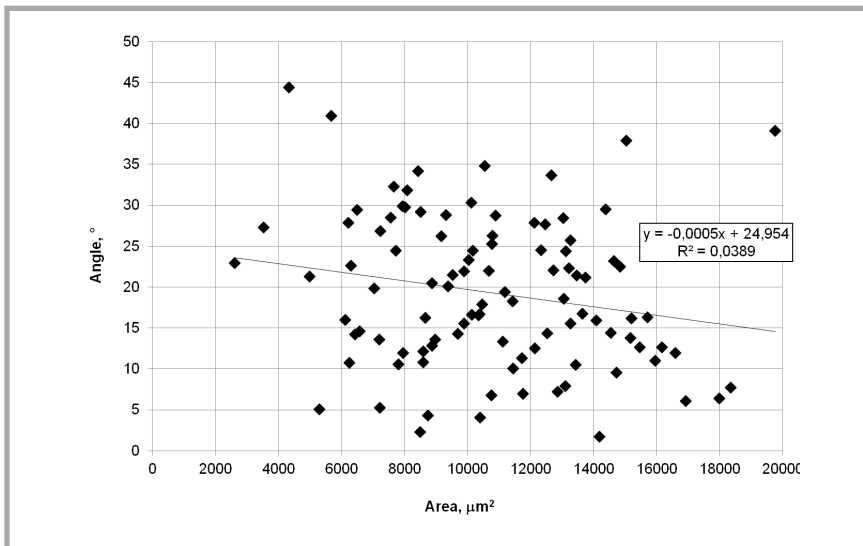


Figure 16. Angle vs. area of spacings measured for fabric 91.

cameras, 126 spacings were visualised, but only 100 of which were measured. Table 2 presents the results of both the area and angle measurements. The mean spacing area of the fabric is defined as the ratio of the spacing and the total image areas calculated directly from the image using simple segmentation (2D analysis described above) [4]. The mean value of this parameter was obtained by averaging results from the left and right images.

Histograms of the areas and angles are presented in Figure 15. Both figures show large deviation from the mean value, which can be caused either by the fabric properties themselves or/and by the operator, who was not very precise in selecting and marking the same points in both the left and right images.

Moreover the high standard deviation of the measurement strongly depends on the size of the spacings measured. The uncertainty analysis presented above indicates that the relatively large value of standard deviation of the area and angle measurements is due deviation in the size and orientation of the spacings in the fabric. In order to apply this measurement system in practice, it is necessary to improve its accuracy. One should not forget that the overall accuracy of the system is determined by the spatial resolution of the cameras, the accuracy of the calibrator as well as by the operator's ability to select the points in both images. Therefore to achieve better performance, we recommend to repeat the measurements and average the results. It seems that 8 - 10 consecutive results of the measure-

ment are enough, and can increase the accuracy significantly.

A plot of the orientation angle versus the area of the spacing is shown in Figure 16, confirming the very small or even lack of correlation between these quantities. In other words, according to expectations, the size of the spacing between yarns has a very little or no impact on the frontal orientation of the channel in the fabric.

## Conclusions

The stereovision system presented in this paper was constructed and used to measure the 3D geometrical properties of fabrics. Theoretical analysis and preliminary measurement results confirmed the usefulness of standard 2-camera stereo imaging for measuring the area and angle of the front of the spacing in between yarns in a fabric on a micro scale. The accuracy of the system, equipped with standard CCD cameras, zoom lens and extender tube, was sufficient to measure the area of spacings with a diameter of about 200 µm. The accuracy of measuring the angle was worse. In order to measure the orientation of the channel, we recommend averaging the results of 8 - 10 measurement sessions. The system allows to make statistics of areas and angles measured in the 3D space. In the future, the system proposed will be used for measuring and correlating the geometrical properties of fabrics obtained from 3D analysis with moisture, vapor, air and, if possible, with the radiation transfer rate. For this aim we intend to

elaborate a new expert system and artificial neural network. However, it must be emphasised that the main efforts in the future will concentrate on the automation of the entire measurement using reference points in both images as well as on-line matching procedures.

## References

1. Hatze H. High-precision three-dimensional photogrammetric calibration and object space reconstruction using a modified DLT-approach. *J. Biomech* 1988; 21: 533-538.
2. Sitek Z. *Fotogrametria ogólna i inżynierska*. Ed. Państwowe Przedsiębiorstwo Wydawnictw Kartograficznych im. Eugeniusza Romera, Warszawa-Wrocław, 1991.
3. Istook CL, Hwang S. 3D Body Scanning Systems with Application to the Apparel Industry. *Journal of Fashion Marketing and Management* 2001; 5, 2: 120-132.
4. Wilbik-Halgas B, Danych R, Wiecek B. Establishing the course and wale density of knitted fabrics by a computer analysis of 2D images. *Fibres & Textiles in Eastern Europe* 2006; 14, 5: 107-110.
5. McLoughlin, J. Chapter 13: Automated fabric inspection. In: Fairhurst C. *Advances in apparel production*. Ed. Woodhead, London, 2008.
6. Bye E, McKinney E. Fit analysis using live and 3D scan models. *International Journal of Clothing Science and Technology* 2010; 22, 2/3: 88-100.
7. Solomon Ch, Breckon T. *Fundamentals of Digital Image Processing: A Practical Approach with Exp. in Matlab*. Ed. Wiley-Blackwell, 2010.
8. Power EJ, Apeagyei PR, Jefferson AM. Integrating 3D Scanning Data & Textile Parameters into Virtual Clothing. In: *2nd International Conference on 3D Body Scanning Technologies*. Hometrica Consulting, Lugano, Switzerland, 2011, pp. 213-224.
9. Parker JR. *Algorithms for Image Processing and Computer Vision*. Second Edition, Wiley, 2011.
10. Rzeszotarski D. Reconstruction methods for 3D scenes from stereoscopy. *Pomiary Automatyka Kontrola (PAK)* 2013; 9: 977-980.
11. DLT Method, <http://www.kwon3d.com/theory/dlt/dlt.html>.
12. Evaluation of measurement data — Guide to the expression of uncertainty in measurement, JCGM 100: 2008.
13. [http://www.bipm.org/utis/common/documents/jcgm/JCGM\\_100\\_2008\\_E.pdf](http://www.bipm.org/utis/common/documents/jcgm/JCGM_100_2008_E.pdf)
14. [TC]² <http://www.tc2.com>.

Received 21.02.2014 Reviewed 24.07.2014